

## Conduction-electron spin density around Fe impurities in Cu above and below the Kondo temperature\*

James B. Boyce<sup>†</sup> and Charles P. Slichter

*Department of Physics and Materials Research Laboratory, University of Illinois, Urbana, Illinois 61801*

(Received 10 March 1975)

We have observed the nuclear resonances of five shells of Cu atoms which are near neighbors to single Fe impurities in dilute alloys of CuFe. Each of the satellite shifts are linear in external magnetic field from 7 to 63 kG, and three have positive shifts while two have negative shifts. From line shape, intensity, and width, four of these satellites are identified as being due to the first, second, third, and fourth shells of neighbors. The satellite shifts, which are proportional to the conduction-electron spin density, are compared with the predictions of various theories in order to determine the values of the parameters involved in characterizing dilute magnetic alloys. It is found, using the theory of Jena and Geldart, that a good explanation of the spin density cannot be given unless the crystal-field splitting of the Fe *d* levels is taken into account. The energy-level parameters obtained are: the crystal-field splitting, 0.5 eV; virtual level width, 0.7 eV; Coulomb splitting, 5.6 eV. The magnetization distributed in the electron gas is shown to be aligned antiferromagnetically with the moment on the Fe atom and to be about nine times smaller than this moment. Four of the satellites were observed down to well below the 29-K Kondo temperature, and, in each case, the shift scaled as  $1/(T + 29)$ . Thus, the spin density has the same temperature dependence as the bulk susceptibility, showing that contrary to some speculation there is no drastic change in the spatial polarization associated with the Kondo condensation.

### I. INTRODUCTION

Considerable experimental and theoretical effort has been devoted to determining the behavior of isolated magnetic impurities in nonmagnetic host metals.<sup>1-4</sup> Of particular interest is the nature of the electronic spin state of dilute magnetic alloys that exhibit the Kondo effect. One would like to know the state of the impurity *d* electrons and the form of the correlations of their spins with the spins of the conduction-electron gas, both above and below the Kondo temperature  $T_K$ . A quantity that can yield such information is the conduction-electron spin density  $\sigma(r, T)$ . This is the response of the spins of the conduction-electron gas at position *r* relative to the impurity, and at temperature *T*, to the polarization of the magnetic atom by an external magnetic field *H*. It is analogous to charge density, except that the charge of the particle is replaced by the component of its spin along the applied field  $s_{zi} \delta(\vec{r}_i - \vec{r})$  for the *i*th electron.

Two forms of the spin polarization have been proposed for *H* small enough for a linear response:

$$\sigma(r, T)/H = \chi(T)f(r), \quad (1)$$

$$\sigma(r, T)/H = \chi(T)g(r, T), \quad (2)$$

where  $\chi(T)$  is the spin susceptibility of a single impurity and is often closely fitted by a Curie-Weiss law  $\chi(T) \sim 1/(T + T_K)$ .<sup>4,5</sup> For Eq. (1) the spatial shape of the spin density is given by *f*(*r*) and does not change with temperature both above and below  $T_K$ . In this case only the magnitude of

$\sigma(r, T)$  varies with *T*, and it follows  $\chi(T)$ . The Kondo effect then manifests itself only by the temperature-dependent-to-temperature-independent transition of  $\chi(T)$  as *T* is lowered below  $T_K$ . For Eq. (2) the spatial shape function *g*(*r*, *T*) is also a function of *T*, so the shape changes presumably when *T* is lowered below  $T_K$ , so that  $g(r, T) = f(r)$  for  $T \gg T_K$  but not for  $T < T_K$ . This shape change below  $T_K$  is said to be a manifestation of the formation of the "Kondo condensed state."<sup>4</sup> We shall use this term throughout our paper to signify a condition leading to Eq. (2) as distinguished from Eq. (1).

Both forms of  $\sigma(r, T)$  are predicted theoretically below the Kondo temperature. Müller-Hartmann,<sup>6</sup> using the equation-of-motion method, show that the spin polarization contains only oscillatory terms and supports Eq. (1). On the other hand, Heeger *et al.*,<sup>7</sup> using the Kondo-Appelbaum theory, conclude that Eq. (2) is correct and supported their contention with experiments. Their calculation yields a quasiparticle term which is non-oscillatory and long ranged, but goes to zero far above  $T_K$ . Bloomfield, Hecht, and Sievert,<sup>8</sup> using a two-time thermodynamic Green's functions, conclude that  $\sigma(r, T)$  has a negative definite component, but that it is short range, i.e., extends to about the tenth shell of neighbors. They thus agree with Eq. (2) but disagree in detail with the results of Heeger *et al.*<sup>7</sup>

Above the Kondo temperature the theoretical calculations yield expressions of the form of Eq. (1). There  $\sigma(r, T)$  is given by the well-known

Ruderman-Kittel-Kasuya-Yosida<sup>3</sup> (RKKY) oscillations or, equivalently, the Friedel oscillations.<sup>1</sup> Higher-order perturbation calculations than RKKY have been performed, and they also have the form of Eq. (1).<sup>9</sup> However, RKKY and the higher-order calculations are only valid for  $r$  far from the impurity since they use an exchange-coupling constant that is a  $\delta$  function in real space. Close to the impurity, the magnetic-ion structure and the wave-vector dependence of the scattering are important. This case has been treated by Jena and Geldart<sup>10</sup> and by Alloul.<sup>11</sup> These expressions also have the form of Eq. (1).

Experimentally there is also disagreement as to whether Eq. (1) or Eq. (2) describes the spin density. The alloy considered is the classic Kondo system  $CuFe$ , which has a convenient Kondo temperature of 29 K.<sup>5</sup> Golibersuch and Heeger,<sup>12</sup> comparing Mössbauer data with their NMR linewidth results, conclude that the spin polarization contains a spatially extended term which is aligned ferromagnetically with the local  $d$  spin on the Fe and accounts for one-half the total bulk susceptibility. This spin polarization term goes to zero above about 16 K and 60 kG. The NMR linewidth studies were extended by Potts and Welsh<sup>13</sup> who conclude that below  $T_K$  there is either an enhancement of the spin polarization or a formation of an additional long-range spin polarization. The original Mössbauer results of Steiner *et al.*<sup>14</sup> indicated that a small antiferromagnetic polarization of the electron gas existed and was destroyed above 30 K and 100 kG. Thus these authors supported Eq. (2). We discuss the most recent work of Steiner *et al.* below.

On the other hand, the neutron-diffraction experiments of Stassis and Shull<sup>15</sup> and the NMR wipeout studies of Nagasawa and Steyert<sup>16</sup> yield no long-range nonoscillatory spin polarization or spin-density enhancement below  $T_K$ . Also Alloul, Darville, and Bernier<sup>17</sup> show that the NMR linewidth due to single Fe impurities scales with  $\chi(T)$ . These experiments thus agree with Eq. (1).

We have measured  $\sigma(r, T)$  at four distinct shells of neighbors to isolated Fe atoms in  $CuFe$  from well below  $T_K$  to well above  $T_K$ , and find Eq. (1) is correct. A preliminary report of this work has already appeared.<sup>18</sup>

We have obtained the spin density at Cu neighboring sites to single Fe impurities by observing the shift of their weak satellite resonances from the main Cu resonance both above and below  $T_K$ . This satellite NMR technique has been useful in obtaining  $\sigma(r, T)$  in dilute magnetic alloys since the Cu nuclei interact with this conduction-electron spin density via the contact hyperfine interaction which produces an NMR frequency shift

proportional to  $\sigma(r, T)$ . Satellites which are magnetically shifted from the main line resonance have been observed in several dilute alloys. Satellite studies done below the characteristic temperature only have been performed by Alloul *et al.* on  $AlMn$ ,<sup>19</sup> and by our group on  $CuNi$ ,<sup>20</sup>  $CuCo$ ,<sup>21</sup> and  $CuV$ .<sup>22</sup> Satellite studies above  $T_K$  only have been done by Karnezos and Gardner<sup>23</sup> and Tompa<sup>24</sup> on  $CuMn$  and by Boyce, Aton, and Slichter<sup>22</sup> on  $CuMn$  and  $CuCr$ .

In Sec. II we discuss the experimental techniques. In Sec. III the experimental results are presented and discussed as is a simple explanation of why Eq. (1) turns out to be correct. The results are summarized and conclusions drawn in Sec. IV.

## II. EXPERIMENTAL METHOD

### A. Sample preparation

The alloys were prepared from 99.999% pure Cu and 99.95% pure Fe. These starting materials were melted together in an induction furnace at 1200–1250 °C for about 1 h and quenched from the melt. The resulting ingot was swaged to less than 50% of its initial diameter and given a homogenization anneal at about 1050 °C for 3–4 days. This annealed ingot was rapidly quenched into ice water to minimize precipitation in this poor metallurgical system. The samples were powdered with a tungsten-carbide rotary cutter and only the 400-mesh powder used in the experiments. Chemical analysis determined the Fe concentrations of the samples used to be 0.5, 0.1, 0.083, and 0.05 at. %. A multielement mass-spectrographic analysis was performed on all samples to insure that extraneous impurity contamination was negligible. Electron microprobe analysis on the 0.5% sample showed that the alloys were homogeneous to within  $\pm 5\%$  of the chemically analyzed concentration. One of the samples (0.1%) was stored at liquid-nitrogen temperature. But a run at 300 K on this sample showed no difference in the satellite positions compared with the other alloys which were kept at room temperature.

### B. Experimental apparatus and procedure

#### 1. Cross-coil rig

Some of the runs were performed using a Varian crossed-coil rf unit with field modulation. The output of this rf unit went to a lock-in amplifier (PAR HR-8) operating at 197 Hz. The dc field was swept and successive passes were made through the resonance and averaged in a Nicolet 1072 signal averager. The audio- and rf-frequency, amplitude, and phase stability of this rig was such as to allow unattended runs of about 24 h with negli-

gible drifts. Temperature and dc field drifts during this period were also negligible. These long averaging times were needed in searching for and detecting the very weak satellite resonances.

This apparatus was used for runs between 7 and 15 kG and at fixed temperatures of 77, 210, and 300 K. At the low temperatures the sample was frozen in mineral oil inside a small Dewar that fit into the crossed-coil probe. The temperatures were measured using a copper-Constantan thermocouple placed near the sample.

### 2. Single-coil coaxial bridge apparatus

This rig is similar to that described previously.<sup>21</sup> It contains all broad-band rf components with bandwidths greater than 10–100 MHz. This wide-band feature facilitated the study of the satellites over the large dc field range of 9 to 63 kG. This field was supplied by a Westinghouse superconducting solenoid which was fitted with a Janis variable-temperature Dewar. The Dewar was operated over the temperature range of 1.4–330 K. This temperature was measured and controlled using a GaAs diode mounted near the sample. The magnetic field induced error in the GaAs diode was reproducible and easily corrected for. The temperature was held constant to within a few tenths of a degree or better so that drifts would have a negligible effect on the satellite widths and positions.

### 3. Common experimental procedures

For both spectrometers the satellite shifts were measured by shifting the rf frequency and noting the position of the Cu main line resonance in the alloy with the dc field and field sweep unchanged. This technique of measuring the satellite shifts and the external dc field is sufficiently accurate due to the very small change in the main line Knight shift in the CuFe alloy compared with pure Cu.<sup>25, 26</sup>

The positions of the satellites were taken as the zero crossing of the derivative of the absorption signal assuming a reasonable baseline. This technique is quite accurate (see Fig. 1) except for very wide satellites and for satellites close to the main line where in both cases the baseline is somewhat uncertain. The rf phase adjustment required to observe satellites close to the main resonance<sup>20</sup> introduced an additional position uncertainty. These uncertainties, however, are much smaller than the shifts and are estimated in the size of the error bars.

In most cases, to enhance the signal-to-noise ratio, a lock-in time constant (TC) large enough to shift the resonance position, but not so large

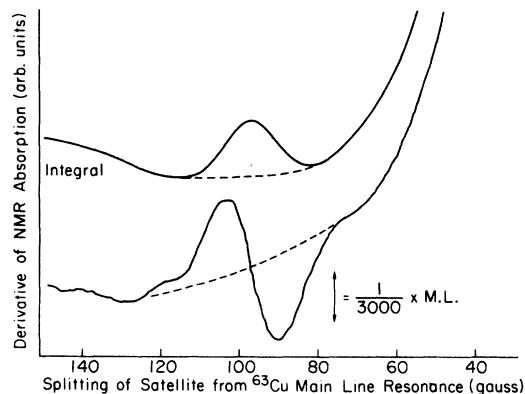


FIG. 1. Satellite B of the  $^{63}\text{Cu}$  main line resonance in Cu-0.05-at. % Fe at 298 K and 35.3 kG. The lower trace is the average of 109 sweeps of the derivative of the absorption signal. The arrows show the scale relative to the main line (ML) peak-to-peak intensity. The upper trace is the integral of this signal performed digitally with the signal averager. The dashed curves are the estimated baselines.

as to severely distort the line shape was used. This shift was always smaller than the linewidth. A TC-shift correction was then obtained by measuring the shift of the main line as a function of TC with the field sweep rate ( $dH/dt$ ) kept the same as for the satellite resonance. Then, assuming the same line shape for satellite and main line, the ratio of the shift to the width is a function of the product of  $dH/dt$  with the ratio of the time constant to the width. This relation was applied to both satellite and main line to obtain the TC shift of the satellite resonance.

## III. EXPERIMENTAL RESULTS AND DISCUSSION

### A. Measurement of spin density

The host NMR spectrum consists of a large main line resonance signal due to atoms far from the impurity plus weak satellite signals due to atoms near the impurity. The main line resonance of CuFe has been thoroughly studied by others.<sup>7, 12, 13, 17, 25, 26</sup> Its Knight shift is not changed from that of pure Cu, but its width is greatly broadened by the oscillatory conduction-electron spin density due to the Fe impurities. We are concerned here with the satellite spectra in CuFe.

The satellites have their NMR field shifted from that of the main line owing to changes in the conduction-electron spin density  $\sigma(r, T)$ , and owing to changes in the conduction-electron charge density  $\rho(r, T)$  resulting from the presence of the impurity. Since these changes fall off rapidly with distance from the impurity, only the near shells of neighbors are shifted sufficiently in field to be observed

as satellites to the main line. The near-neighbor satellite shift can be separated into two parts: the magnetic shift due to  $\sigma(r, T)$  which is linear in the external magnetic field  $H$  and the electric quadrupole shift due to  $\rho(r, T)$ . The quadrupole shift will be field independent if it is first order and will vary as  $1/H$  if it is second order. This assumes  $H$  is small enough so as not to cause a change of the Kondo state. We find that the magnetic shift dominates in  $\text{CuFe}$  as is expected for this magnetic alloy.

Figure 1 shows a typical satellite to the  $\text{Cu}^{63}$  main line. The lower trace is the derivative of the absorption signal and the upper trace is the integral of this experimental curve. The dashed line is the estimated baseline. This baseline has been properly determined since the zero crossing of the derivative and the peak of the integral coincide.

Five such satellite resonances were observed and their positions as a function of external magnetic field have been measured. This field dependence at 300 K is shown in Fig. 2. The three satellites on the high-field side of the main line resonance are labelled *A*, *B*, and *C* and the two on the low field side *M* and *N*. All the splittings are linear in external magnetic field for all the temperatures and fields studied, showing that the electric

quadrupole effects are small and that we have not induced any changes of state by the application of  $H$ .

Since the magnetic shift dominates, the experimental shift is a measure of  $\sigma(r, T)$ . The additional field at the nucleus at positions  $r$  relative to the impurity and at temperature  $T$ ,  $\delta H(r, T)$ , is related to  $\sigma(r, T)$  by the equation

$$\Delta K(r, T) = \delta H(r, T)/H = -\frac{2}{3}\pi\gamma_e\hbar\sigma(r, T)/H.$$

The minus sign in the above equation occurs because the spin and the moment of the electron have the opposite sign. Note that  $\delta H$ , the extra field at the nucleus produced by the spin polarization, is related to  $\Delta H$ , the amount the magnet must be shifted for an experiment at fixed frequency to go from the main line to the satellite, by the relation  $\delta H = -\Delta H$ . Now the Knight shift in the pure host is given by  $K = \frac{2}{3}\pi\langle|\psi(0)|^2\rangle_{E_F}\chi_s$ , where  $\chi_s$  is the spin susceptibility of the conduction electrons in the pure host and  $\langle|\psi(0)|^2\rangle_{E_F}$  is the average of the wave-function density at a nucleus for states at the Fermi energy. So by taking the ratio of  $\Delta K$  and  $K$  we get

$$\frac{\Delta K(r, T)}{K} = -\frac{\gamma_e\hbar}{\chi_s}\frac{\sigma(r, T)}{\langle|\psi(0)|^2\rangle_{E_F}H}. \quad (3)$$

Thus  $\Delta K/K$  is proportional to  $\sigma(r, T)/H$  with constants of proportionality which are properties of pure copper, and thus are independent of  $r$  and  $T$ . The quantities  $\Delta K/K$  at 300 K for each of the satellites are listed in Fig. 2. For satellite *A* a direct dipole-dipole contribution is included so that the isotropic part to be compared with Eq. (3) is  $\Delta K/K|_A = -5.24 \pm 0.3$  at 300 K.

The splittings are independent of concentration for the concentrations studied: 500, 830, 1000, and 5000 ppm. The intensity of the satellites varies nearly linearly with concentration, showing that they arise from single Fe impurities, not pairs or larger clusters. The fact that no satellites due to pairs or larger clusters were observed is to be expected for two reasons. First, the number of pairs or clusters in a dilute alloy of concentration  $c$  is expected to be smaller than the number of singles by roughly a factor of  $c^m$ , with  $m \geq 1$ . So the number of clusters is much smaller than the number of singles at low concentrations. Second, there are many ways to form a cluster of a given size thus lowering the number of identical clusters. So the intensity of a satellite due to a cluster should be much smaller than the intensity of a satellite due to a single. We see satellites due to single impurities only and so are measuring single-impurity effects.

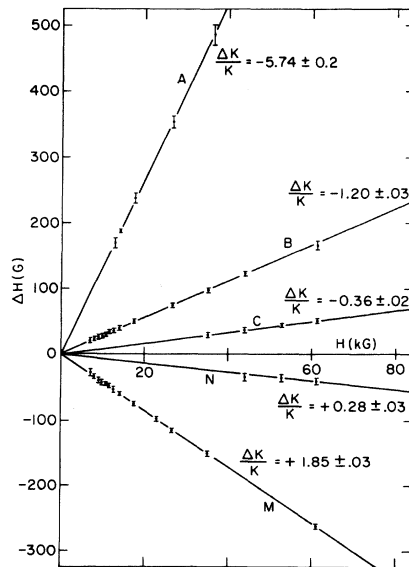


FIG. 2. Magnetic field dependence of satellite separations from main  $\text{Cu}^{63}$  resonance at 300 K. Shift of satellite  $H$  in gauss from the  $\text{Cu}^{63}$  resonance vs applied field  $H$  in kilogauss. The  $\Delta K/K$  for satellite *A* includes a direct dipole-dipole contribution of  $-0.5 \pm 0.1$  so that the isotropic part of  $\Delta K/K|_A = -5.24 \pm 0.3$ .

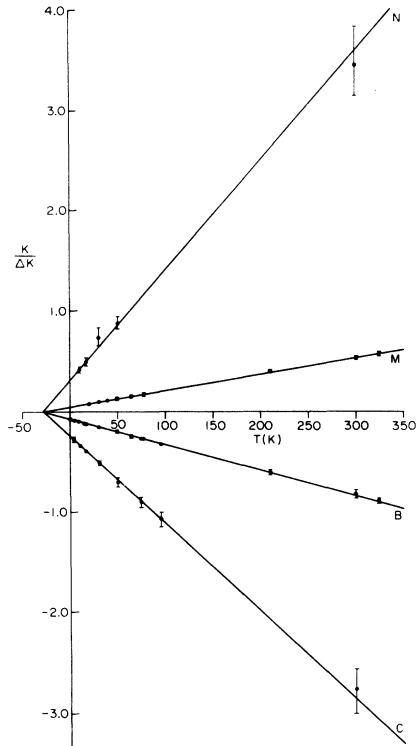


FIG. 3.  $(\Delta K/K)^{-1}$  vs temperature for four of the satellite resonances. The straight lines are least-squares fits to the data, and the temperature intercepts are the same within experimental error and approximately equal to  $-29$  K.

## B. Temperature dependence of spin density in CuFe

### 1. Satellite NMR results

In connection with the Kondo effect, the temperature dependence of  $\sigma(\nu, T)$  is of the most interest, i.e., how does  $\sigma(\nu, T)$  change on going below the Kondo temperature of 29 K. To determine this, the satellite shifts were measured to below 29 K. The widths of all the satellites increased with decreasing temperature (see Fig. 5) and, as a result, satellite A was not observed at or below 77 K. However, the other four satellites were followed down to below  $T_K$ . Satellite B was observed down to 1.4 K at 9.5 kG and down to 17 K at 24 kG. Satellite M was followed down to 20 K at 9.5 kG and down to 30 K at 24 kG. All splittings are linear in field in contrast to the linewidth results.<sup>13</sup> Satellite C was followed down to 4.2 K at 24 kG and N to 10 K at 24 kG. Most of the data below 77 K was taken on the 830-ppm sample. A few points at 24 kG on satellite B, C, M, and N and at 9.5 kG on B were done on the 500-ppm sample. Satellites B and M were observed at 64 K and 24 kG on the 5000-ppm sample.

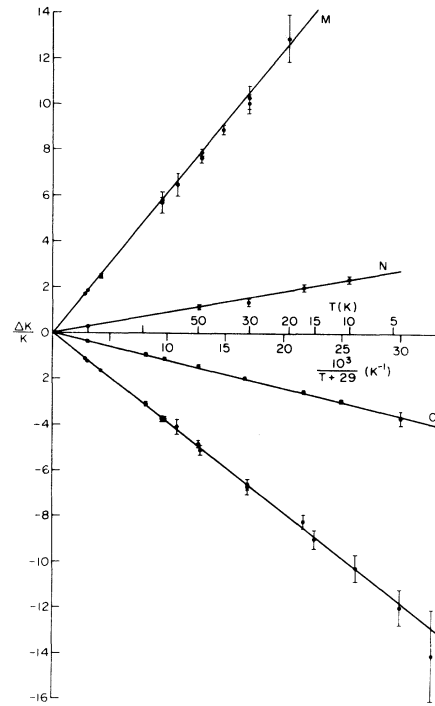


FIG. 4. Knight shifts vs  $1/(T+29)$  for four of the satellites. No additional polarization is seen to form below  $T_K=29$  K.

According to Eq. (3),  $\Delta K(\nu, T)/K \propto \sigma(\nu, T)/H$ , so the temperature dependence of  $\Delta K/K$  tells how  $\sigma(\nu, T)/H$  varies with temperature at each of the neighboring lattice sites  $\nu$  for which a satellite was observed. If  $\Delta K/K$  fits a Curie-Weiss law,  $1/(T+\Theta)$ , a plot of the reciprocal of  $\Delta K/K$  vs  $T$  would yield a straight line with a temperature intercept at  $-\Theta$ , where  $\Theta$  is the Curie-Weiss temperature. Figure 3 is such a plot of  $(\Delta K/K)^{-1}$  vs  $T$ . The straight lines, which are least-squares fits to the data, obey a Curie-Weiss law with  $\Theta$ 's listed in Table I. Each of the  $\Theta$ 's is the same within experimental error, and they are the same as the Curie-Weiss  $\Theta$  of  $29 \pm 1$  K determined from the bulk susceptibility measurements of Tholence and Tournier.<sup>5</sup>  $\Delta K/K$  is plotted versus  $1/(T+29)$  in Fig. 4 to emphasize the low-temperature ( $\leq T_K$ ) points. The fact that the straight lines fit the data shows that  $\Delta K/K$  has the same temperature dependence as  $\chi(T)$  both above and below  $T_K$ .

We therefore conclude that Eq. (1) describes the results, and that the entire manifestation of the Kondo effect on  $\sigma(\nu, T)$  is through its effect on the susceptibility, causing the magnetic-to-non-magnetic transition of  $\chi(T)$  as  $T$  is lowered below  $T_K$ . There is no shape change of  $\sigma(\nu, T)$ , no additional spin polarization below  $T_K$ , and there is no additional spin compensating electron cloud below  $T_K$ .

TABLE I.  $\theta$ 's from a least-squares fit to a  $1/(T+\theta)$  law of the temperature dependence of the shifts of each of the satellite resonances in Fig. 3. Also listed is the  $\theta$  from the static susceptibility measurements (Ref. 5).

Satellite	$\theta$ ( $^{\circ}$ K)
A	...
B	$29.2 \pm 2.4$
C	$27.6 \pm 4.0$
M	$29.2 \pm 2.3$
N	$29.3 \pm 7.1$
Bulk susceptibility	$29 \pm 1$

These results agree with the neutron-diffraction studies of Stassis and Shull<sup>15</sup> and the recent NMR linewidth studies of Alloul *et al.*<sup>17</sup> They disagree, however, with some of the conclusions of the earlier NMR linewidth experiments<sup>12, 13</sup> and the earlier Mössbauer studies.<sup>14</sup> But we think that these disagreements can be reconciled by a reinterpretation of the data of these conflicting studies.

## 2. NMR linewidth studies

The NMR linewidth results, which support the formation of a Kondo condensed state below  $T_K$ , may possibly be brought into agreement with our results by considering the effect of clusters. As first pointed out by Tholence and Tournier,<sup>5</sup> clusters of two or more Fe atoms have a lower  $T_K$  than singles and make a large contribution to the susceptibility. Since the satellite splittings are spectroscopic measurements, they pick out only one kind of species—in this case isolated Fe atoms. But linewidths should include effects of pairs and larger clusters as shown by Lang *et al.*<sup>21</sup> in the case of CuCo. Potts and Welsh<sup>13</sup> have published extensive data on the linewidth versus concentration of Fe for the CuFe system. Since they do not propose that clusters explain their data, it is a safe bet that their data do not fit such an interpretation precisely. Nevertheless, one knows that clusters contribute to susceptibility, and thus must contribute to the linewidth. Lang, Boyce, Lo, and Slichter<sup>21</sup> showed quantitatively that clusters provide the explanation of a comparable anomaly in CuCo. Before seeking other interpretations for CuFe one should at least first correct for the clusters. Using the data of Tholence and Tournier<sup>5</sup> one gets that at 4.2 K for a sample of 280 ppm, half the low-field susceptibility comes from singles, half from pairs (if we take the pairs as having a  $T_K \ll 4.2$  K). At this temperature, Potts and Welsh find that the linewidth (actually what they call  $S_L$ ) of their 305-ppm sample is  $(1.75 \pm 0.3)$  times larger than the value one deduces for singles from a high-temperature extrapolation. Since

Lang, Boyce, Lo, and Slichter<sup>21</sup> show that, to a good first approximation, the linewidth contribution scales with the susceptibility contribution, we see that much of the Potts and Welsh anomalous linewidth at low temperatures must come from pairs.

Following the arguments of Ref. 21, the concentration of singles,  $c_1$ , is

$$c_1 = c(1-c)^Z, \quad (4)$$

where  $Z$  is the number of neighbor sites which, if occupied by an impurity, change the center from a single to a pair. If we assume a similar situation for pairs, then the concentration of pairs,  $c_2$ , is

$$c_2 = Zc^2(1-c)^{Z'}, \quad (5)$$

where  $Z'$  is the number of neighboring sites to the pair which, if occupied, convert the pair to a triple. Similar expressions can be obtained for larger clusters.

The contribution to the main resonance linewidth of a cluster is, to a good approximation, proportional to the concentration of that cluster times its magnetization, assuming a broadening mechanism of the form of Eq. (1), an assumption which appears to be valid from our satellite results. We make the further assumption that the broadening of the linewidth is due mainly to singles and pairs of impurities, with the contribution of larger clusters being relatively small. From the susceptibility results,<sup>5</sup> this is a reasonable assumption. We also ignore the distinction between ferromagnetically and antiferromagnetically aligned pairs.<sup>5</sup> Then, in low enough external magnetic fields so that the pair magnetization is not saturated, the slope of the main line broadening versus field is

$$S_L = A \frac{c(1-c)^Z}{T+\Theta} + B \frac{Zc^2(1-c)^{Z'}}{T+\Theta_2}, \quad (6)$$

where  $A$  and  $B$  are constants independent of  $c$  and  $T$ , and  $\Theta$  and  $\Theta_2$  are the Curie-Weiss temperatures of singles and pairs, respectively, with  $\Theta = 29$  K for CuFe. As shown by Lang *et al.*,<sup>21</sup>  $A$  and  $B$  should be similar in magnitude. Tholence and Tournier<sup>5</sup> state that for CuFe  $Z = 520$  for pairs and  $0 < \Theta_2 < 5$  K. Let us take  $\Theta_2 = 1$  K and assume that  $Z' = Z$ . Then Eq. (6) with these parameters ( $Z' = Z = 520$ ,  $\Theta = 29$  K,  $\Theta_2 = 1$  K) can be compared with the data of Potts and Welsh.<sup>13</sup> With  $A = 61$  K and  $B = 14.4$  K, a reasonably good fit is obtained. At 1.65 K, Eq. (6) fits the concentration dependence of the experimental  $S_L$  to within 10% (the approximate experimental uncertainty of Ref. 13) and at 4.2 K to within 15%. This is for  $c$  between 90 and 1260 ppm (Fig. 5, Ref. 13). Also the temperature

dependence of  $S_L$  from 1.65 to 77 K (Fig. 9, Ref. 13) is fit to within about 15% by Eq. (6). Thus the anomaly in the temperature dependence of the linewidth of CuFe (Fig. 9, Ref. 13) can be attributed to interactions.

It is interesting to note that despite the complicated concentration dependence of Eq. (6), it is linear in  $c$  to within about 15% (the experimental uncertainty) for  $c$  between 90 and 1260 ppm at 1.65 and 4.2 K and for the values of the parameters listed above. As a result one cannot conclude that the linearity of  $S_L$  in  $c$  implies the absence of interactions.

It would be surprising if the above simple model involving only singles and pairs could completely explain the NMR linewidth results in CuFe, especially in view of the fact that the difficult metallurgical problems of these systems make it difficult to remove effects of sample history, and thus put into question expressions based on random distributions. Nevertheless, we continue to see how the parameters found for low fields work at high fields. The expression obtained from Eq. (6) for the slope of the linewidth broadening versus  $H$  at high fields, where the pair contribution has saturated, is

$$S_H = A c(1 - c)^Z / (T + \Theta) . \quad (7)$$

This equation does not fit the data well for the values of the parameters mentioned above. For example, the experimental ratios of  $S_L/S_H$  at 1.65 and 4.2 K are  $1.91 \pm 0.3$  and  $1.75 \pm 0.3$ , respectively (Fig. 6, Ref. 13), whereas Eqs. (6) and (7) yield values of 1.4–2.8 at 1.65 K and 1.2–2.0 at 4.2 K for  $c$  between 300 and 1260 ppm. Also Alloul *et al.*<sup>17</sup> experimentally obtain an equation for  $S_H$  similar to Eq. (7), but with  $Z = 0$  instead of 520 and with  $A \approx 47$  K (for Lorentzian broadening) instead of 61 K. The high-field results of Potts and Welsh<sup>13</sup> yield Eq. (7) with  $Z = 0$  and  $A \approx 44$  K. However, the disagreement on the detailed form of  $S_H$  does not invalidate the general conclusions drawn above concerning  $S_L$ : (i) the approximate linearity in  $c$  does not necessarily imply one is observing effects due to singles, and (ii) the low-temperature anomaly in  $S_L$  can be due to interaction effects and is not necessarily due to a change in the shape of  $\sigma(r, T)$ . Alloul *et al.*,<sup>17</sup> discussing their host NMR results, arrive at similar conclusions. Hence we believe the early NMR linewidth studies do not conflict with our results.

### 3. Mössbauer studies

Steiner, Zdrojewski, Gumprecht, and Hufner<sup>14</sup> published highly precise Mössbauer studies giving an interpretation which appeared at first glance

to disagree with our results. We pointed out<sup>18</sup> that their data, together with earlier Mössbauer data of other workers,<sup>27</sup> could in fact be brought into agreement with our own if one recognized that Steiner *et al.*<sup>14</sup> were basing their interpretation on combining their data with that of earlier workers. Either their data or the earlier data taken *alone* agreed with our results but appeared to disagree with each other as to the high-temperature limiting value of the Mössbauer shift. Subsequently, Campbell<sup>28</sup> published a paper, followed by a reply from Steiner and Hufner,<sup>29</sup> discussing the high-temperature limit.

Recently, however, Steiner, Hufner, and Zdrojewski<sup>30</sup> have published new data and a new analysis in which they conclude that there is a disagreement between their data and earlier data. They then find their data gives the same result as we have, i.e., that Eq. (1) is correct. In the process they conclude that the best value of  $T_K$  is  $27.6 \pm 1.0$  K using one method and  $28.2 \pm 1.0$  K by another. These results are seen to agree with the stated errors with Table I. Thus we believe the Mössbauer data support our conclusions.

We should comment on the  $T^2$  dependence of the shift observed by Steiner *et al.*<sup>14</sup> Such a temperature variation is expected on theoretical grounds<sup>31</sup> but only at temperatures well below a characteristic temperature of the order of  $T_K$ . From the Mössbauer data this occurs below 10 K. Unfortunately in this temperature region our satellite results are not sufficiently accurate nor is there sufficient data to observe a deviation from a  $1/(T + \Theta)$  law. However, our data are not in conflict with the beautiful results of Steiner *et al.*<sup>14</sup>

### C. Identification of satellites

Identification of which shell of neighbors gives rise to a given satellite is possible in principle if one uses single crystals. The dependence of satellite position and intensity as a function of the orientation of the magnetic field with respect to the crystal axes permits identification of the shell. Stakelon in our laboratory has used this method to show that satellite *B* is the third-neighbor shell. He has shown that a satellite similar to *A* is the first neighbor in CuCo. By "similar" we mean (i)  $\Delta K/K$  scales nearly in the ratio of the susceptibilities of Co vs Fe; (ii) as discussed below, the satellite possesses an observable structure in the powder, the only satellite for either magnetic atom to do so. Thus satellite *A* is almost surely the first neighbor.

Further information is available to make a tentative identification of other satellites. This information is contained in the lineshape, width, and relative intensity of the satellite resonances.

### Line shape of satellite A

Satellite A at room temperature exhibits the asymmetric lineshape characteristic of a direct or pseudodipole interaction between a Cu shell of neighbors and the Fe moment. This lineshape is similar to that observed by Lang *et al.*<sup>21</sup> for the first neighbor in CuCo and is shown in their Fig. 1. In his single-crystal studies, Stakelon shows that at the first-neighbor site in CuCo the pseudodipolar coupling is about twice as big as the direct dipolar. The coupling is much larger at the first neighbor than at any other observed site.

Since the satellite A in CuFe is the only satellite to display the asymmetric line shape, it has the largest combined dipolar-plus-pseudodipolar coupling and is probably the first neighbor. Assuming a susceptibility of  $9.5 \times 10^{-27}$  emu/atom for the iron susceptibility at 300 K,<sup>32</sup> we account for the asymmetry of satellite A if we assume satellite A is a first neighbor with a combined pseudopolar-plus-direct-dipolar coupling about twice the direct-dipolar coupling alone. This agrees reasonably with the result for CuCo.

### 2. Relative intensity of satellites

The intensity of the resonances gives another clue towards the identification of the satellites. For a dilute alloy, which is a true solid solution, the intensity  $I$  of a satellite due to a shell of neighbors containing  $n$  atoms is related to the intensity  $I_0$  of the main line resonance by

$$I = ncI_0. \quad (8)$$

$n$  is listed for the first ten shells of neighbors in Table II. However, unlike the situation in CuMn,<sup>23</sup> Eq. (8) yields satellite intensities in CuFe which are larger than those observed. A similar situation was observed in CuCo. The reasons for this are probably related to clustering of some of the impurities in CuFe and CuCo which, unlike CuMn, do not form good solid solutions. These clusters do not give rise to observable satellites and so Eq. (8) yields values of  $I$  which are too large. Even replacing  $c$  by the number of singles  $c_1$  from Eq. (4) gives intensities which are too large for the low-concentration alloys, indicating that there are more clusters in CuFe than given by assuming a purely random distribution of impurities.

Despite this, the ratio of the intensities of the satellite resonances for a given alloy is equal to the ratio of the  $n$ 's for the corresponding shells. These ratios for each of the satellites with respect to satellite M are 2 for A, 2.2 for B, 1.8 for C, and about 1 for N. The errors in these ratios are approximately  $\pm 30\%$ . These ratios were obtained from the room-temperature data where the widths are not too large and the signal-to-noise ratio is best. The differences in the widths were taken into account. The large uncertainty in these relative intensities is due mainly to the problems in determining the correct baseline. Using these intensities, we obtain an approximate identification of the satellites by referring to the values of  $n$  in Table II and assuming that the satellites with the largest shifts are closest to the impurity and that they are within the first eight shells. We then

TABLE II. Comparison of the experimental and various theoretical results for  $\Delta K/K$  at 300 K. The theoretical expressions are evaluated for the first ten shells of neighbors around the Fe impurity. The RKKY result is from Eq. (21) with  $J_{\text{eff}} = -2$  eV. The Jena and Geldart expression (Ref. 10) is evaluated from Eqs. (27') and (28') where the crystal-field splitting has been taken into account and with the values of the parameters listed in Eq. (29). The asymptotic expression is determined in the same way but with  $\Lambda^{\sigma}(r) = 1$  and  $\theta^{\sigma}(r) = 0$ . The last column is taken from Table III of Alloul *et al.* (Ref. 17) for  $\Gamma_d^{\uparrow} = \Gamma_d^{\downarrow} = \frac{1}{6}E_F$ .

Shell	Number of sites, $n$	$r$ (Å)	Experiment (satellite)	$\Delta K/K$ at 300 K			Alloul <i>et al.</i>
				RKKY ( $J = -2$ eV)	Jena and Geldart with crystal-field splitting	Asymptotic expression	
1	12	2.55	$-5.24 \pm 0.3$ (A)	5.80	-5.28	6.84	-5.29
2	6	3.61	$1.85 \pm 0.03$ (M)	-2.52	1.78	1.89	2.35
3	24	4.42	$-1.20 \pm 0.03$ (B)	1.28	-1.41	-2.07	-0.30
4	12	5.10	$-0.36 \pm 0.02$ (C)	0.28	-0.34	1.69	-1.01
5	24	5.71	$[0.28 \pm 0.03$ (N)]	-0.68	0.21	0.94	-0.04
6	8	6.25		-0.18	0.10	-1.02	0.32
7	48	6.75		0.36	-0.12	-0.58	-0.03
8	6	7.22		0.26	0.12	-0.02	-0.31
9	36	7.66		-0.08	0.09	0.56	-0.22
10	24	8.07		-0.24	0.02	0.24	0.03

have that  $A$  is the first neighbor,  $M$  is the second, and  $B$  and  $C$  are from the third, fourth, and fifth shells, with  $B$  most likely the third and  $C$  most likely the fourth. The uncertainty in the intensity of satellite  $N$  make its identification too difficult to estimate.

### 3. Width of satellites

The satellite widths as a function of temperature and field yield further information toward the identity of the satellite resonances as well as to possible spin-lattice relaxation processes. By width we mean the peak-to-peak width in gauss of the derivative of the absorption signal. These widths have been measured down to low temperatures for satellites  $B$ ,  $C$ ,  $M$ , and  $N$ .  $N$ 's width is too uncertain owing to its proximity to the main line to be discussed, so only  $B$ ,  $C$ , and  $M$  will be considered. The widths of  $B$  and  $M$  at low temperatures were measured at 9.5 and 24 kG and of  $C$  at 24 kG only. Most of the data were taken on the 830-ppm sample, but some were also taken on the 500-ppm sample. No significant difference in the widths for the 500- and 830-ppm samples was detected within the large experimental error. The widths increased with field but slower than linearly. The widths increased with decreasing temperature faster than  $1/(T+29)$ , but lower than  $1/T$ . The widths as a function of temperature for satellites  $B$ ,  $C$ , and  $M$  at 24 kG in the 830-ppm sample are shown in Fig. 5. The large error bars are due to the uncertainty in the proper choice of baseline. The baseline uncertainty has a much larger effect on the width determination than it does on the position.

To obtain the broadening of the satellite resonance due to the impurity,  $\Delta W_{\text{sat}}$ , one must deconvolute the pure host contribution to the measured width. But for the satellite widths much larger than the pure copper width of 7 G, this is a negligible correction.<sup>26</sup> So  $\Delta W_{\text{sat}}$  is equal to the measured width within the large experimental error.

We assume a Lorentzian broadening<sup>26</sup> so that the total width is the sum of the contributions from each of the broadening mechanisms. Then

$$\Delta W_{\text{sat}} = \Delta W_{\text{quad}} + \Delta W_{\text{dipole}} + \Delta W_{\text{interaction}} + \Delta W_{T_1} \quad (9)$$

$\Delta W_{\text{quad}}$  is the contribution due to the electric quadrupole interaction in these powdered alloys. We assume that the first-order quadrupole coupling wipes out all but the  $\text{Cu } +\frac{1}{2}$  to  $-\frac{1}{2}$  transition, so that  $\Delta W_{\text{quad}}$  is the second-order broadening of this transition. This term should be small compared with the other terms since it is proportional to  $1/H$ , whereas the widths increased with  $H$ .  $\Delta W_{\text{dipole}}$

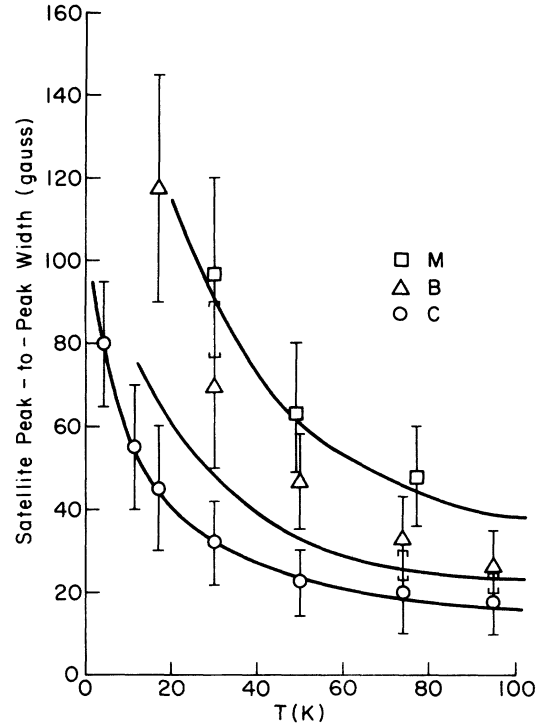


FIG. 5. Peak-to-peak widths of satellites  $B$ ,  $C$ , and  $M$  at 24 kG as a function of temperature in the 830-ppm sample. The solid lines are fits to the data using Eq. (13) with the parameters of Eq. (14) with  $B$  the third neighbor,  $C$  the fourth, and  $M$  the second. The fit to  $M$  and  $C$  is good, whereas the fit to  $B$  is too low. This poor fit to  $B$  is to be expected from the single crystal results of T. Stakelon, as discussed in the text. The fit to the data on  $B$  and  $M$  at 9.5 kG is similar.

is the contribution from the direct dipole-dipole and the pseudodipolar interaction. It is the same interaction as is responsible for the asymmetry in satellite  $A$  and is proportional to  $\chi(T)H/r^3$ .

$\Delta W_{\text{interaction}}$  is the width due to a distribution in the size of the moments on the Fe impurity due to interactions with other impurities<sup>3</sup> plus the width due to the overlap of the spin-density oscillations from other impurities. This second part is the same as the impurity-induced broadening of the main line,  $\Delta W_{\text{ML}}$ . The relative importance of the first part is not known, and a careful concentration dependence would be required to determine it. Only 500- and 830-ppm samples were studied. The fact that the widths were not too different in these two samples indicates that this first part of  $\Delta W_{\text{interaction}}$  may not be very large. So we will assume that only the second part is significant:

$$\Delta W_{\text{interaction}} \approx \Delta W_{\text{ML}} \quad (10)$$

The last term in Eq. (9) is a lifetime broadening of the satellite resonances due to their fast relaxa-

tion rates. It is made up of four terms<sup>33</sup>:

$$\gamma \Delta W_{T_1} + 1/T_1|_{\text{GH}} + 1/T_1|_{\text{TD}} + 1/T_1|_{\text{LD}} + 1/T_1|_{\text{BGS}} , \quad (11)$$

where  $\gamma$  is the Cu gyromagnetic ratio. The GH term<sup>34</sup> is due to an interaction of the Cu neighbors with the impurity via a virtual excitation of the spin density and is expected to be small.<sup>33</sup> Transverse and longitudinal fluctuations of the Fe moment couple to the Cu neighbors via the direct and indirect dipole interaction and give rise to the TD and LD contributions, respectively. We know from our single-crystal studies that there is significant pseudodipolar coupling in addition to direct dipolar coupling. Roughly, the pseudodipolar goes as  $\cos(2k_r r + \phi)/r^3$ , where  $\phi$  is some approximate phase angle. For purposes of linewidth analysis, we focus on the  $1/r^3$  effect since we cannot do otherwise with the data presently available, and since the precision of the data does not justify too refined an analysis in any event. The TD mechanism is negligible, being much smaller than the Benoit, DeGennes, and Silhouette term,<sup>35</sup> which is due to a mutual spin flip-flop of the Fe electronic spin and the Cu nuclear spin interacting via the spin density. This BGS contribution is small in high external magnetic fields since it does not conserve Zeeman energy. So the only term in Eq. (11) that may be significant at high magnetic fields is  $1/T_1|_{\text{LD}}$ . To obtain a fast temperature dependence as the data require, we assume  $1/T_1|_{\text{LD}}$  has the same form as for paramagnetic impurities in insulators with  $\gamma H \tau \ll 1$ :

$$\frac{1}{T_1}|_{\text{LD}} \propto \frac{1}{r^6} \tau \propto \frac{1}{r^6} \frac{1}{T} , \quad (12)$$

where  $\tau$  is the spin-lattice relaxation time of the Fe moment and has the form<sup>33</sup>

$$\tau T = c ,$$

where  $c$  is a constant. The fact that the LD mechanism dominates and has the free-spin form of Eq. (12) is consistent with the conclusions of Potts and Welsh<sup>13</sup> from experiments on the main line  $T_1$  of CuFe.

Equation (9) then becomes

$$\begin{aligned} \Delta W_{\text{sat}} &\simeq \Delta W_{\text{dipole}} + 1/\gamma T_1|_{\text{LD}} + \Delta W_{\text{ML}} \\ &\simeq A_1 \frac{1}{r^3} \frac{H}{T+29} + A_2 \frac{1}{r^6} \frac{1}{T} + \Delta W , \end{aligned} \quad (13)$$

where  $A_1$  and  $A_2$  are constants independent of  $r$ ,  $H$ ,  $T$ , and  $c$ . A fairly reasonable fit of the experimental widths to Eq. (13) can be obtained with satellites  $M$ ,  $B$ , and  $C$  being the second, third, and fourth neighbors, respectively. The values

of the constants are then

$$A_1 = 5 \times 10^{-24} \text{ cm}^3 \text{ K}$$

and

$$A_2 = 2 \times 10^{-42} \text{ cm}^6 \text{ K G} . \quad (14)$$

The solid curves in Fig. 5 are Eq. (13) with the above parameters and  $\Delta W_{\text{ML}}$  has been estimated from the data of Potts and Welsh.<sup>13</sup> The fits to  $M$  as the second neighbor and  $C$  as the fourth neighbor are good, while the fit to  $B$  as the third neighbor is not as good. A good fit is obtained for  $B$  with a radius between that of the second and third neighbors. Note, however, that we know  $B$  is the third neighbor. This larger width of satellite  $B$  is consistent, however, with the CuFe single-crystal studies of Stakelon who finds a large anisotropic coupling for satellite  $B$  but not for satellite  $M$ . Such a coupling has been ignored in Eq. (13), which should thus yield too small a width for  $B$  and the correct width for  $M$  and  $C$  as observed in Fig. 5.

We should obtain a theoretical estimate of  $A_1$  and  $A_2$  to compare with the values obtained from a fit to the data, Eq. (14). We have that

$$\Delta W_{\text{dipole}} = \xi \frac{\chi H}{r^3} = \xi \frac{\mu_{\text{eff}}^2}{3k_B(T+29)} \frac{H}{r^3} , \quad (15)$$

where  $k_B$  is the Boltzmann constant,  $\mu_{\text{eff}}$  is the effective Fe moment, and  $\xi$  is a constant of order unity that depends in detail on the ratio of  $\chi H/r^3$  to the width of a Gaussian broadening function for the satellite and includes the fact that there is both dipolar and pseudodipolar coupling. So comparing Eqs. (13) and (15) and using  $\mu_{\text{eff}} = 3.4 \mu_B$ ,<sup>5</sup> we obtain

$$A_1 = \xi \frac{\mu_{\text{eff}}^2}{3k_B} = 2.4 \times 10^{-24} \xi \text{ cm}^3 \text{ K} . \quad (16)$$

Comparing Eq. (16) with  $\xi \approx 1$  to Eq. (14), we see that our experimental value of  $A_1$  is reasonable. The fact that the value of  $A_1$  in Eq. (14) is a factor of two larger than the value obtained from the susceptibility results in Eq. (16), is similar to the situation observed with the line shape of satellite  $A$ . There the dipolar coupling constant is two times larger than that obtained from  $\chi$  again as a result of the pseudodipolar coupling.

An estimate of  $A_2$  can be obtained from the expression for the relaxation rate due to paramagnetic impurities:

$$\begin{aligned} 1/\gamma T_1|_{\text{LD}} &= 3 \sin^2 \theta \cos^2 \theta \gamma \tau (\mu_{\text{eff}}^2/r^6) \xi^2 \\ &= 3 \sin^2 \theta \cos^2 \theta \gamma c \mu_{\text{eff}}^2 (1/r^6) (1/T) \xi^2 . \end{aligned}$$

Comparing this with Eq. (13), we have, assuming direct dipolar coupling,

$$A_2 \sim \gamma \mathfrak{C} \mu_{\text{eff}}^2 \xi^2 = 7 \times 10^{-36} \mathfrak{C} \xi^2 \text{ (sec K) cm}^6 \text{ K G} . \quad (17)$$

For  $\tau T \xi^2 = \mathfrak{C} \xi^2 \sim 3 \times 10^{-7} \text{ sec K}$ , Eq. (17) agrees with the experimental value for  $A_2$  in Eq. (14). The precise value of  $\mathfrak{C}$  is not known, but its value is expected to be between  $10^{-11}$  and  $10^{-8}$ . For example, using the expression from perturbation theory on the  $s$ - $d$  Hamiltonian<sup>4</sup> with a reasonable exchange-coupling constant ( $J_{sd} \sim 0.5 \text{ eV}$ ),<sup>37</sup> yields  $\tau T \sim 10^{-11} \text{ sec K}$ . Potts and Welsh<sup>13</sup> obtain  $\tau T \sim 10^{-10} \text{ sec K}$  from their main line  $T_1$  data. Allou and Bernier,<sup>33</sup> from their main line  $T_1$  studies assuming  $\xi \cong 1$ , obtain  $\tau T \sim 10^{-9} \text{ sec K}$  in  $\text{CuMn}$  and  $\text{CuCr}$  if the LD mechanism dominates. The temperature-dependent component of the transmission electron-spin-resonance linewidth yields  $\tau T = 4.5 \times 10^{-9} \text{ sec K}$  for  $\text{CuCr}$ , and  $\tau T = 2.5 \times 10^{-8} \text{ sec K}$  for  $\text{CuMn}$ .<sup>33</sup> The various estimates of  $\mathfrak{C}$  thus range from  $10^{-11}$ – $10^{-8} \text{ sec K}$ . Stakelon's results from single crystals show that the total dipolar coupling is about 3 times bigger than the direct dipolar, giving  $\xi \cong 3$ . Thus we estimate  $T\tau \cong 3 \times 10^{-8} \text{ K sec}$  from our value of  $A_2$ . In addition the  $1/(T + \theta_2) = 1/(T + 1)$  term due to pairs in  $\Delta W_{\text{interaction}}$  may also enhance the theoretical value for  $A_2$ . So our experimental value of  $A_2$  may not be too unreasonable, and a better theoretical determination of the widths and a better knowledge of the parameters involved are required to draw firm conclusions.

Combining all the above information on the identification of the satellites, we have the following tentative assignment:  $A$  is the first neighbor,  $M$  the second,  $B$  the third, and  $C$  the fourth. This is in agreement with the single-crystal studies of  $T$ . Stakelon who concludes that  $M$  is the second and  $B$  is the third. The information on satellite  $N$  is too uncertain to make an identification.

#### D. Spatial dependence of $\sigma(r, T)$

With the above assignment of the satellite resonances, one may compare the values of  $\Delta K/K$  with the various theoretical expressions. In the following we will use

$$\langle S_z \rangle = - \frac{\chi(T)H}{g\mu_B} = - \frac{\mu_{\text{eff}}^2 H}{3g\mu_B k_B(T+29)} , \quad (18)$$

where  $\langle S_z \rangle$  is the thermal average of the Fe spin. We will also assume that  $g=2$ , so that

$$\mu_{\text{eff}} = 3.4 \mu_B = g\mu_B [S(S+1)]^{1/2}$$

yields a spin  $S$  of approximately 1.25.<sup>5</sup>

First let us consider the RKKY expression for the spin density<sup>3</sup>:

$$2\sigma(r) = \delta n^\uparrow - \delta n^\downarrow = -9\pi(J_{sd}/E_F) \langle S_z \rangle F(2k_F r) , \quad (19)$$

where  $E_F$  and  $k_F$  are the Fermi energy and wave vector of pure Cu,

$$F(x) = (x \cos x - \sin x)/x^4 ,$$

and  $J_{sd}$  is the exchange-coupling constant in the  $s$ - $d$  Hamiltonian:

$$\mathcal{H} = 2J_{sd} \sum_i \vec{S} \cdot \vec{s}_k \delta(\vec{r}_i) . \quad (20)$$

Then combining Eq. (19) with Eqs. (3) and (18) gives

$$\frac{\Delta K}{K} \Big|_{\text{RKKY}} = 4\pi S(S+1) \frac{(-J_{sd})}{k_B(T+29)} F(2k_F r) , \quad (21)$$

where we have used the free-electron expression for the conduction-electron spin susceptibility,  $\chi_s = 3 \mu_B^2 / 2E_F$ . The value of  $J_{sd}$  determined from the 29-K Kondo temperature is about  $-0.4 \text{ eV}$ .<sup>36</sup> Blandin<sup>37</sup> has shown that it is more appropriate to use

$$J_{\text{eff}} = (2l+1)J_{sd} \simeq -2 \text{ eV}$$

instead of  $J_{sd}$  when  $d$ -wave scattering ( $l=2$ ) rather than  $s$ -wave scattering is involved. Allou *et al.*<sup>17</sup> obtain approximately this value for  $J_{\text{eff}}$  from their NMR linewidth studies (their definition of  $J$  is twice our's). So using  $-2 \text{ eV}$  for  $J_{sd}$  in Eq. (21), we obtain the values of  $\Delta K/K_{\text{RKKY}}$  at 300 K listed in Table II. It is seen that the magnitude of  $\Delta K/K$  is approximately correct but that the sign is opposite. The fact that the sign is wrong is consistent with the results of Jena and Geldart.<sup>10</sup> The fact that the correct magnitude is obtained is perhaps fortuitous since the RKKY expression applies only at large distances from the impurity. This is supported by the fact that RKKY predicts that some of the further out neighbors should also be observable but were not seen.

An expression that applies in close to the impurity as well as in the asymptotic region has been obtained by Jena and Geldart.<sup>10</sup> Using the Friedel-Anderson model they obtain

$$2\sigma(r, T) = [\delta n^\uparrow(r) - \delta n^\downarrow(r)] \langle S_z(T) \rangle / S , \quad (22)$$

with

$$\delta n^\sigma(r) = -30 [\Lambda^\sigma(r)/(2k_F r)^3] \sin \delta_d^\sigma(E_F) \times \cos[2k_F r + \delta_d^\sigma(E_F) + \theta^\sigma(r)] \quad (23)$$

and

$$\tan \delta_d^\sigma(E_F) = \Gamma_d^\sigma / (E_d^\sigma - E_F) . \quad (24)$$

Here  $\Gamma_d^\sigma$  and  $E_d^\sigma$  are the width and position, respectively, of the spin-up and spin-down resonant

levels in the Anderson model. As a first approximation

$$\begin{aligned}\Lambda^\sigma(r) &\approx 1 + \gamma^\sigma / k_F r, \\ \theta^\sigma(r) &\approx \eta^\sigma / k_F r,\end{aligned}\quad (25)$$

so that in the asymptotic region  $\Lambda^\sigma(\infty) = 1$  and  $\theta^\sigma(\infty) = 0$ . Then Eq. (23) reduces to the usual asymptotic expression of Daniel and Friedel.<sup>38</sup> In Eq. (25)

$$\begin{aligned}\gamma^\sigma &= -(E_F / \Gamma_d^\sigma) \sin^2 \delta_d^\sigma(E_F), \\ \eta^\sigma &= \frac{17}{2} - \frac{6}{1 + (q^*/k_F)^2} + \frac{E_F}{\Gamma_d^\sigma} \sin \delta_d^\sigma(E_F) \cos \delta_d^\sigma(E_F),\end{aligned}\quad (26)$$

where  $q^*$  is the sum of the Thomas-Fermi screening wave vector and the reciprocal of the extent of the Fe  $d$ -wave function ( $q^* = 6.3/\text{Å}$ ). The approximation also requires in the dilute limit that  $\Gamma_d^\dagger = \Gamma_d^\dagger$ . Combining Eqs. (18) and (22)–(26) with Eq. (3) yields

$$\frac{\Delta K(r, T)}{K} = - \frac{\mu^2}{3gS\chi_s k_B(T+29)} [\delta n^\dagger(r) - \delta n^\ddagger(r)].$$

Using  $\mu_{\text{eff}} = 3.4\mu_B$ ,  $g = 2$ ,  $S = 1.25$ ,<sup>5</sup> and  $\chi_s = 1.55 \times 10^{-29}$  emu/atom,<sup>39</sup> this equation becomes

$$\frac{\Delta K(r, T)}{K} = - \frac{6.2 \times 10^4}{T+29} [\delta n^\dagger(r) - \delta n^\ddagger(r)]. \quad (27)$$

In order to compare the above expressions with experiment, one needs the resonant level widths and positions. For these we use the Friedel sum rule<sup>1</sup>:

$$\begin{aligned}\delta_d^\dagger(E_F) + \delta_d^\ddagger(E_F) &= \frac{1}{5} \pi N, \\ \delta_d^\dagger(E_F) - \delta_d^\ddagger(E_F) &= \frac{1}{5} \pi 2S.\end{aligned}\quad (28)$$

Here  $N$  is the number of  $d$  electrons on the Fe impurity and  $S = 1.25$  from the susceptibility results.<sup>5</sup> If  $N$  and  $\Gamma_d (= \Gamma_d^\dagger = \Gamma_d^\ddagger)$  are known, then Eqs. (23)–(28) yield  $\Delta K/K$ . We have attempted to fit our experimental  $\Delta K/K$ 's at 300 K by varying these two unknown parameters over a physically reasonable range. No good fit could be obtained. This might suggest that something that is physically important has been left out of the above expressions.

Evidence that this is the case comes from the single-crystal NMR experiments of Stakelon. He finds that in  $\text{CuCo}$  there is a pseudodipolar interaction between the Co and the first-neighbor Cu nuclei which is not axially symmetric about the Cu-Co internuclear vector. This result fits the symmetry of the site about this axis (it is a twofold axis), however an axially symmetric result would be found if one could neglect all atoms other

than the Co and the Cu whose nucleus is under study. Thus the crystal potential must play a role.

In pure Cu, evidence for the role of the crystal potential arises from the fact that Bloch waves rather than plane waves are needed to account for the size of the Knight shift, and from the fact that experimentally the Fermi surface is not a sphere in  $k$  space.

One effect of the crystal potential will be to split the fivefold angular degeneracy of the iron  $d$  electrons. This effect can readily be included in the Jena-Geldart theory in the following simple way. Addition of a crystal potential will give both diagonal and off-diagonal matrix elements of the Jena-Geldart Hamiltonian. The diagonal elements will simply shift energy levels. The off-diagonal elements would be present even in pure Cu, for which they would be responsible for converting plane waves into Bloch waves. We assume the same result occurs with an impurity atom. As is well known, using the Bloch waves enhances the theoretical Knight shift by several orders of magnitude over the free-electron value. We expect a similar enhancement will occur with an impurity atom, and that in computing the ratio  $\Delta K/K$  the enhancement will cancel out.

Consequently, we believe it to be a fair starting point to assume the crystal potential simply shifts energies but that free-electron basis states may still be used. Our procedure for modifying the Jena-Geldart results is then as follows:

First, instead of having two fivefold degenerate virtual levels centered at  $E_d^\sigma$ , one has four virtual levels centered at  $E_{d(t)}^\sigma$  and  $E_{d(e)}^\sigma$ .  $E_{d(t)}^\sigma$  refers to the threefold degenerate  $t_{2g}$  orbitals ( $xy$ ,  $xz$ ,  $yz$ ) and  $E_{d(e)}^\sigma$  refers to the twofold degenerate  $e_g$  orbitals ( $x^2 - y^2$ ,  $3z^2 - r^2$ ). The  $e_g$  orbitals lie above the  $t_{2g}$  orbitals in energy and their splitting is  $\Delta$ , the crystal-field splitting. We take the widths of all four virtual levels to be the same and the Coulomb splittings of the  $t_{2g}$  and  $e_g$  orbitals to be the same. So we have the following energy-level parameters:

$$\begin{aligned}\Delta &= E_{d(e)}^\dagger - E_{d(t)}^\dagger = E_{d(e)}^\ddagger - E_{d(t)}^\ddagger, \\ U &= E_{d(e)}^\ddagger - E_{d(e)}^\dagger = E_{d(t)}^\ddagger - E_{d(t)}^\dagger, \\ \Gamma &= \Gamma_{d(t)}^\dagger = \Gamma_{d(t)}^\ddagger = \Gamma_{d(e)}^\dagger = \Gamma_{d(e)}^\ddagger.\end{aligned}$$

The second modification of the Jena-Geldart theory due to the crystal-field splitting is to weight the spin density due to scattering from the  $t_{2g}$  and  $e_g$  orbitals differently in different crystal directions. These weighting factors,  $W_e(\vec{r})$  and  $W_t(\vec{r})$ , take into account the different directional dependence of the  $t_{2g}$  and  $e_g$  orbitals and give rise to the experimentally observed anisotropy in the single-crystal experiments.  $W_e(\vec{r})$  and  $W_t(\vec{r})$  are readily

calculated for the neighboring shells of atoms with the known directional dependence of the  $t_{2g}$  and  $e_g$  orbitals and with the normalization condition that  $W_e(\vec{r}) + W_t(\vec{r}) = 1$ .

With the above modifications due to the crystal-field splitting Eq. (27) becomes

$$\frac{\Delta K}{K}(\vec{r}, T) = -\frac{6.2 \times 10^4}{(T+29)} \{ W_t(\vec{r}) [\delta n_t^\uparrow(r) - \delta n_t^\downarrow(r)] + W_e(\vec{r}) [\delta n_e^\uparrow(r) - \delta n_e^\downarrow(r)] \}, \quad (27')$$

where  $\delta n_t^\sigma(r)$  and  $\delta n_e^\sigma(r)$  are given by Eqs. (23)–(26) with the inclusion of the  $t$  and  $e$  subscripts on the phase shifts. The Friedel sum rule of Eq. (28) is also modified:

$$\begin{aligned} \delta_{d(t)}^\uparrow(E_F) + \delta_{d(t)}^\downarrow(E_F) &= \frac{1}{3} \pi N_{(t)}, \\ \delta_{d(e)}^\uparrow(E_F) + \delta_{d(e)}^\downarrow(E_F) &= \frac{1}{2} \pi N_{(e)}, \\ \delta_{d(t)}^\uparrow(E_F) - \delta_{d(t)}^\downarrow(E_F) &= \frac{1}{3} \pi 2S_{(t)}, \\ \delta_{d(e)}^\uparrow(E_F) - \delta_{d(e)}^\downarrow(E_F) &= \frac{1}{2} \pi 2S_{(e)}, \\ N &= N_{(t)} + N_{(e)}, \quad S = S_{(t)} + S_{(e)}. \end{aligned} \quad (28')$$

Using  $S = 1.25$  from the susceptibility results<sup>5</sup> and the assumptions that  $U$  is the same for the  $t_{2g}$  and  $e_g$  levels,  $\Delta$  is the same for the spin-up and spin-down levels, and  $\Gamma$  is the same for all levels, the number of unknown parameters in Eqs. (27') and (28') reduces to three:  $\Gamma$ ,  $N_{(e)}$ , and  $S_{(e)}$ , or, equivalently,  $\Gamma$ ,  $U$ , and  $E_{d(e)}^\uparrow$ . These parameters were varied over a physically reasonable range and a good fit to the Knight-shift data at 300 K was obtained. Only the shifts for satellites  $A$ ,  $M$ ,  $B$ , and  $C$  (1st, 2nd, 3rd, and 4th neighbors) were used since the assignment of satellite  $N$  is uncertain. The parameters so obtained are

$$\begin{aligned} \Gamma &= 0.71 \text{ eV}, \quad U = 5.6 \text{ eV}, \quad \Delta = 0.52 \text{ eV}, \\ E_{d(t)}^\uparrow &= 0.19 E_F, \quad E_{d(t)}^\downarrow = 0.99 E_F, \\ E_{d(e)}^\uparrow &= 0.26 E_F, \quad E_{d(e)}^\downarrow = 1.06 E_F, \\ S &= 1.25, \quad S_{(t)} = 0.62, \quad S_{(e)} = 0.63, \\ N &= 7, \quad N_{(t)} = 4.5, \quad N_{(e)} = 2.5. \end{aligned} \quad (29)$$

The total spin on the Fe atom was fixed at 1.25.<sup>5</sup> The fit yielded a total of seven  $d$  electrons on the Fe atom corresponding to one of the two  $s$  electrons on the isolated Fe atom going into the Cu conduction band and the other into the Fe  $d$  band. Gardner and Flynn<sup>40</sup> obtained a slightly different value of 6.4 electrons on the Fe  $d$  level. The value of  $U/\Gamma = \beta > 1$  is consistent with CuFe being magnetic in the Anderson sense, and a level width of 0.71 eV is in rough agreement with estimates made from other experiments.<sup>4</sup> The value of the

crystal-field splitting is comparable to the virtual level width, as it should be for crystal-field effects to be important.

The values of  $\Delta K/K$  determined from Eq. (27') with the parameters of Eq. (29) are listed in Table II in the column labelled Jena and Geldart. For comparison we have also listed in the adjacent column the asymptotic results obtained in the same manner but with  $\Lambda^\sigma(r) = 1$  and  $\theta^\sigma(r) = 0$ , the Daniel-Friedel expression. It is seen that the asymptotic expression is way off and of the opposite sign as the data in some cases.<sup>10</sup> The Jena-Geldart results with crystal-field splitting are seen to fit the data quite well, deviating at most by 15% at the third neighbor. In addition, it is seen that the experimental shift of satellite  $N$  is best fit by the calculated value for the fifth neighbor. Since the calculated values of  $\Delta K/K$  were obtained by fitting only to the first four neighbor shifts, one may possibly conclude that satellite  $N$  is the fifth neighbor. Also, it should be noted that the calculated  $\Delta K/K$ 's for the sixth through tenth neighbors are  $\leq 0.12$ . This is not within the experimental resolution and so is consistent with the fact that only the first five shells of neighbors were observed as resolved satellites to the main line.

We believe that our results illustrate physically the way in which a crystalline potential introduces angular dependence into the spin density. A better theoretical grounding is needed before one can have an estimate of how seriously to take the numerical results.

Another calculation of  $\Delta K/K$  has been performed by Alloul *et al.*<sup>17</sup> Their results are deduced from the Hartree-Fock magnetic limit of the Anderson model with values of  $E_d^\sigma$  determined from Eqs. (24) and (28) with  $N=7$  and  $S=1.25$ . They neglect crystal-field effects. Different widths,  $\Gamma_d^\uparrow = \Gamma_d^\downarrow$ , were tried and a best fit was obtained by Alloul *et al.*<sup>17</sup> for  $\Gamma_d^\uparrow = \Gamma_d^\downarrow = \frac{1}{6} E_F$ . Their results are listed in Table II. There is good agreement for the first, second, and sixth neighbors. Very good agreement between this calculation and experiment would be obtained if our assignments for satellites  $B$  and  $C$  were reversed. Then  $B$  would be the fourth rather than the third neighbor, and  $C$  would be the sum of the third and eighth rather than the fourth. But this assignment would be inconsistent with the data on the satellite widths and, more importantly, would be inconsistent with the single-crystal results of Stakelon who determined  $B$  to be the third neighbor.

#### E. Total magnetization in electron gas

There has been some disagreement about the total magnetization in the conduction-electron gas induced by the Fe impurity below  $T_K$ . Stassis and

Shull<sup>15</sup> have concluded that the additional conduction-electron magnetization in the electron gas,  $\Delta\chi_{\text{gas}}(T)H$ , is between 10 and 35% of the total magnetization per Fe impurity  $\chi(T)H$ . Golibersuch and Heeger,<sup>12</sup> on the other hand, conclude that half the total magnetization is localized on the impurity and half is in the electron gas. However, their calculations were based on the Kondo-Appelbaum theory which later was shown to have difficulties.

Our experiments can deduce the conduction-electron magnetization at sites other than the central atom. We assume that the magnetization on a neighbor atom at distance  $r_i$ ,  $\Delta\chi_s(r_i, T)H$ , is related to the magnetization on an atom of pure copper,  $\chi_s H$ , by the relation

$$\Delta\chi_{\text{gas}}(r_i, T) = \chi_s \Delta K(r_i, T)/K. \quad (30)$$

By summing over the neighbors, we can get the conduction-electron magnetization outside the central cell  $\Delta\chi'_{\text{gas}}(T)$ . Taking  $n_i$  atoms in the  $i$ th shell,

$$\Delta\chi'_{\text{gas}}(T) \approx \chi_s \sum_i n_i \frac{\Delta K(r_i, T)}{K}. \quad (31)$$

Using  $\chi_s = 1.55 \times 10^{-29}$  emu/atom,<sup>39</sup> we obtain

$$\Delta\chi'_{\text{gas}}(t) \approx (-12\%) \chi(T). \quad (32)$$

So the magnetization in the electron gas outside the central cell is aligned antiferromagnetically relative to the magnetization localized on the Fe atom and is roughly nine times smaller than the magnetization on the Fe. This is in approximate agreement with Stassis and Shull.<sup>15</sup> The perturbation-theory results<sup>1</sup> predict that the integral of  $\sigma(r, T)$  over  $r$  is  $2J_{sd} \rho_1 \langle S_z \rangle$ , where  $\rho_1$  is the density of states per spin at the Fermi surface (0.146/eV). Using Eqs. (18) and (30) with  $g=2$ , perturbation theory then implies that

$$\Delta\chi_{\text{gas}}(T) = J_{sd} \rho_1 \chi(T). \quad (33)$$

For  $J_{\text{eff}} = -2$  eV this yields  $\Delta\chi_{\text{gas}}(T) = (-30\%) \chi(T)$ . Comparison of this result with Eq. (32), however, depends on the theory used to relate  $\Delta\chi_{\text{gas}}(T)$  with  $\Delta\chi'_{\text{gas}}(T)$ .

Using this same approach, we may compare our results with the average Knight shift  $\bar{K}$  obtained by Gardner and Flynn<sup>40</sup> in liquid CuFe. They obtain

$$\frac{1}{K} \frac{d\bar{K}}{dc} (1373 \text{ K}) = -15. \quad (34)$$

From our data at 300 K, we have

$$\frac{1}{K} \frac{d\bar{K}}{dc} (300 \text{ K}) \approx \sum_i n_i \frac{\Delta K(r_i, 300 \text{ K})}{K} = -83.$$

Scaling this up to 1373 K using a  $1/(T+29)$  law, we obtain

$$\frac{1}{K} \frac{d\bar{K}}{dc} (1373 \text{ K}) \approx -19,$$

in reasonable agreement with the liquid CuFe result in Eq. (34).

#### F. Simple explanation for correctness of Eq. (1)

The question arises whether or not one can understand why Eq. (1) is correct rather than Eq. (2). We present the following argument.

We consider an impurity such as iron which has a permanent magnetic moment and discuss it in the Anderson model, which lends itself nicely to discussing the spin polarization at neighboring sites. We will first review the usual Anderson treatment of the magnetic susceptibility then turn to a description of the Kondo effect in terms of the Anderson model. Next we show what these ideas lead to for the spin polarization in the vicinity of an impurity.

The density of states in the Anderson model is shown in Fig. 6. Consider the diagram labelled "state A." It shows the parabolic density of states of the conduction electron plus the Lorentzian density of states associated with the impurity atom. The fact that the down-spin resonance occurs below the Fermi energy  $E_F$  causes those states to be nearly full, whereas the up-spin resonance, located above  $E_F$ , contains only a few electrons. Thus state A corresponds to a net down spin on the impurity atom and thus an "up" magnetic moment. State B corresponds to a net up spin and down magnetic moment.

States A and B are degenerate in the absence of an external magnetic field  $H_0$ . Application of a

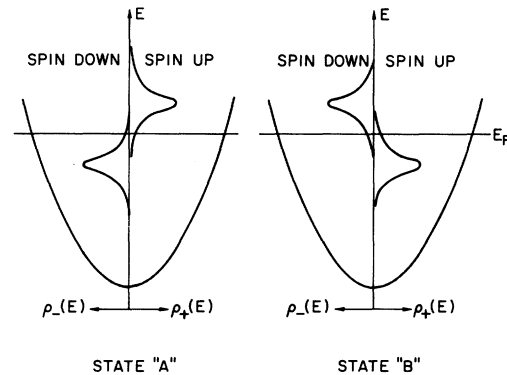


FIG. 6. Density of states in the Anderson model. Showing the densities  $\rho_+(E)$  and  $\rho_-(E)$  of up- and down-spin electrons vs energy  $E$ . The parabolic curves of a free electron are shown as are the extra Lorentzian densities contributed by the magnetic impurity. State A corresponds to an impurity with a net spin down, hence net spin magnetic moment up. State B has a net down-spin and up-spin magnetic moment.

magnetic field produces two effects: (i) it changes state  $A$  and state  $B$  and (ii) it changes the relative likelihood of finding an impurity in the two states.

The change in states  $A$  or  $B$  can be seen by considering state  $A$  only. The Zeeman energy shifts the up-spin and down-spin levels in opposite directions. As a result, there is a repopulation of the up- and down-spin levels. The exact amount of the level shift depends on the size of the Coulomb repulsion  $U$  in the Anderson model. This repopulation effect is what gives rise to the entire magnetic susceptibility of an atom which, in the Anderson model, does not possess a permanent magnetic moment. We expect the resultant magnetization to be nearly temperature independent.

The second effect represents the fact that state  $A$  has a lower magnetic energy than state  $B$  for a magnetic field pointing in the  $+z$  direction. State  $A$  therefore has the larger Boltzmann factor. The resultant magnetization clearly obeys Curie's law in the range of magnetic fields giving linear response.

For iron in copper we neglect the first effect compared to the second.

The Anderson model utilizes the Hartree-Fock approximation. It does not therefore include spin-flip scattering except in terms of the self-consistent populations of the up and down spins. The scattering of a particular spin orientation includes strong scattering as is evidenced by the fact that the scattering resonances are close to the Fermi energy.

In the usual  $s$ - $d$  Hamiltonian used for theoretical treatments of the Kondo effect it is the spin-flip scattering which leads to the divergences. Thus, the Anderson solution does not include the Kondo effect. One needs to go beyond Hartree-Fock to get the effect. If one views the Hartree-Fock solutions as a starting point, one had to include terms which would couple together solutions such as the states  $A$  and  $B$ . As a matter of fact, state  $A$  is really a family of states. This can be seen by starting with  $A$  at absolute zero.  $A$  is a many electron state. At  $T=0$  K it is composed of one-electron states which are full below  $E_F$  and empty above. At  $T>0$  K, some of the one-electron states above  $E_F$  are occupied, some below are empty. We can designate a many-electron state then not only by  $A$  or  $B$  but also by which one-electron states are occupied. For convenience we label these one-electron states:  $A_0, A_1, A_2, \dots$ , etc., with  $A_0$  being the 0-K ground state. These states and

the states  $B_0, B_1, B_2, \dots$  contain many which are either degenerate or nearly degenerate. They are coupled together by the exact Hamiltonian. Resolution of that degeneracy is the heart of the Kondo problem. Presumably the ground state will no longer be  $A_0$ , or  $B_0$ , but some linear combination of the low lying  $A_i$ 's and  $B_i$ 's—mostly from within about  $k_B T_k$  of the ground state. In this regard the situation is much like the BCS theory. In contrast, with BCS, however, it is likely that the ground state is not split off by a gap from the excited states. It is important to realize that the Kondo effect will not have a significant effect on the position or width of the  $d$ -wave scattering resonances, since these properties are determined by chemical considerations (the number of  $d$  electrons the atom should have), energies much larger than the Kondo energies.

At temperatures well above  $T_K$ , we can neglect the Kondo effect. Then the Anderson model should describe things. Application of a magnetic field will cause a preferential alignment corresponding probably to inducing a preponderance of  $A$ -like states.

If  $T \ll T_k$ , there will also be a net magnetization. Whether that arises from a repopulation effect (i.e., occupation of previously unoccupied low-lying states as in the normal spin susceptibility of conduction electrons) or an induced moment effect (admixture of excited states into the ground state as in Van Vleck temperature-independent paramagnetism) we can not say.

As one goes up in temperature, thermal excitation will produce repopulations which progressively break up the Kondo state, leading to the breakdown of the "resolution degeneracy" effects, perhaps in analogy to the way thermal hopping takes over from tunnelling in the problem of diffusion of hydrogen in solids.

What does this picture say about the spin density at neighbor sites? A calculation of spin density can be made in the Anderson model by recognizing that the impurity scatters electrons. The scattering can be described in terms of a phase shift  $\delta_{l\sigma}(k)$ , where  $l$  denotes the angular momentum and  $\sigma$  the spin orientation (up or down) of the scattered wave of the wave vector  $k$ .

In terms of these quantities, one can compute the change in Knight shift at radius  $r$ ,  $\Delta K(r)$  relative to the pure metal  $K$  at temperatures sufficiently far above  $T_K$  for the Anderson model to be valid.

$$\frac{\Delta K(r)}{K} = \frac{\chi}{\chi_s} \{2\pi / [\delta_{2+}(k_F) - \delta_{2-}(k_F)]\} \sum_{\sigma} m_{\sigma} \int \rho_1(W_k) dW_k f(W_k, T) \\ \times \{[n_2^2(kr) - j_2^2(kr)] \sin^2 \delta_{2\sigma}^a(k) - 2n_2(kr) j_2(kr) \sin \delta_{2\sigma}^a(k) \cos \delta_{2\sigma}^a(k)\}, \quad (35)$$

where  $\delta_{2\sigma}^a(k)$  is the  $l=2$  phase shift of spin  $\sigma$  for the  $A$  configuration of Fig. 6,  $n_2$  and  $j_2$  are the usual  $l=2$  spherical Bessel functions,  $\rho_1(W_k)$  the density of conduction-electron states of one spin,  $f(W_k, T)$  the Fermi function, of energy  $W_k$  and temperature  $T$  and zero magnetic field,  $\chi$  is the spin susceptibility of the impurity, and  $\chi_s$  that of the conduction electrons (both on a per atom basis), and  $m_\sigma$  is  $\frac{1}{2}$  or  $-\frac{1}{2}$  spin up or down, respectively. In deriving Eq. (35) we have assumed that only the  $d$ -wave scattering is important in polarizing the spins owing to the fact that the  $d$ -wave phase shifts must be substantial if one is to satisfy the Friedel sum rule for an impurity atom with a partially filled  $d$  shell.  $\delta_{2\sigma}^a(k)$  is  $\frac{1}{2}\pi$  for  $k$  at the center of the  $2\sigma$  resonance, is  $\pi$  well above the resonance, and is zero well below. We have also neglected the repopulation effects within state  $A$  which result from the change in relative position of the up-spin and down-spin resonances. The factor  $\chi$  represents the degree to which the applied field has polarized the impurity and is given by the Boltzmann factor of states  $A$  and  $B$ .

The formula was computed assuming the Anderson model to be valid, but we know that model does not apply below  $T_k$ . We believe a reasonable approximation would be to assume; (i) that we replace the Curie's law  $\chi$  by the Kondo  $\chi$ , and (ii) that we replace  $f(W_k, T)$  by a function  $F(W_k, T)$  which describes the admixture of excited states  $A_1, A_2$ , etc., into the ground Kondo state, much as in the theory of superconductivity there is an admixture of excited electron states of a normal metal in the ground BCS states. Roughly,  $F(W_k, 0)$  should then go from 1 to 0 over a width in energy of order  $k_B T_k$ .

The effect of the  $f$  or  $F$  is to cut off the upper limit of integration near  $E_F$ . The Bessel function terms can be expressed as sums of products of  $(1/kr)^n$ , where  $n=2, 3, 4, 5, 6$  with  $\sin 2kr$  or  $\cos 2kr$ . That  $\Delta K(r)/K$  then generally falls off with distance can be seen as follows: (i) The  $(1/kr)^n$  factors fall off with distance. (ii) Since  $\sin \delta_{2\sigma}^a(k) \cong 0$  when  $k$  is far from the  $\delta_{2\sigma}^a$  resonance, the major contribution from the integrand arises near the resonance.

Far from the impurity, the  $\sin 2kr$  or  $\cos 2kr$  factors oscillate rapidly with  $k$  as one integrates across the scattering resonance, causing the integrand to be alternately positive and negative with  $k$ .

For real systems, the functions  $f$  and  $F$  cut off sharply compared to the width of the scattering resonance. Then, when one is far enough from the impurity so that  $\sin 2kr$  and  $\cos 2kr$  have a number of oscillations as  $k$  crosses the resonances ( $r > 4\pi E_F/k_F \Delta$ , where  $\Delta$  is the level width,  $k_F$  and  $E_F$  the Fermi wave vector and energy) but not far

enough for oscillations across the range of  $k$  corresponding to the cutoff of the functions  $f$  or  $F$  ( $r > 4\pi E_F/k_B T$  or  $r < 4\pi E_F/k_B T_k$ ), the expression leads to the well-known RKKY formula.

If one is a good deal closer to the impurity, there are not enough oscillations to get the RKKY result. But then none of the functions of the integrand change rapidly over the range of  $k$  for which  $f$  or  $F$  go to zero, and the *resultant integral is highly insensitive to the form of the cutoff of  $f$  or  $F$* . Far from the impurity, the total magnetization is small, so that a sharp or slow cutoff of  $F$  does not matter.

We can conclude, then, that the entire manifestation of the Kondo effect on the shape of the spin polarization is through the multiplicative factor of the spin susceptibility.

#### IV. CONCLUSIONS

We have studied the resolved satellite structure due to neighboring shells of Cu atoms around Fe impurities in dilute CuFe alloys. Five satellites were observed and their splittings are linear in field showing that the magnetic interaction dominates and that the quadrupole interaction is small. The satellite intensities scale roughly linearly with concentration indicating that we are measuring effects due to single Fe impurities as is expected with this spectroscopic technique.

From line shape and intensity, we have determined that satellite  $A$  [ $\Delta K/K$  (300 K) =  $-5.24 \pm 0.3$ ] is the first neighbor. From intensity and width the other satellites are identified as follows:  $M$  [ $\Delta K/K$  (300 K) =  $1.85 \pm 0.03$ ] is the second neighbor,  $B$  [ $\Delta K/K$  (300 K) =  $-1.20 \pm 0.03$ ] is the third, and  $C$  [ $\Delta K/K$  (300 K) =  $-0.36 \pm 0.02$ ] is the fourth.  $N$  [ $\Delta K/K$  (300 K) =  $0.28 \pm 0.03$ ] is probably the fifth according to the theoretical calculation. The identification of  $B$  and  $M$  is in agreement with the single-crystal studies of Stakelon.

The widths of satellites  $B$ ,  $C$ , and  $M$  are fit to a model in which the direct dipolar broadening and the longitudinal-dipole relaxation broadening dominate. Satellite  $B$ 's measured width is larger than this model predicts consistent with Stakelon's conclusion that an anisotropic coupling is large for  $B$  but not for  $M$ .

The satellite shifts, which are proportional to the conduction electron spin density, are compared with various theories for  $\sigma(r, T)$ , using the above identification of the satellites. The RKKY expression fits the spatial dependence reasonably well with  $J_{\text{eff}} = -2$  eV, but the sign is wrong in agreement with Jena and Geldart.<sup>10</sup> This fit may be fortuitous since RKKY applies only far from the impurity.

A fit to the Jena-Geldart expression<sup>10</sup> is attempted. A good fit to the data could not be obtained unless the crystal-field splitting is taken into account. With the crystal-field splitting included in the theory the following Anderson-Friedel model parameters are obtained:  $\Delta=0.5$  eV,  $\Gamma=0.7$  eV,  $U=5.6$  eV, and  $N=7$  electrons. The splitting of the two virtual levels and the level width yield a value of  $U/\Gamma=8$ , a value consistent with CuFe being magnetic.  $N$  is equal to 7 implying that one of the two  $s$  electrons in the atom has entered the Fe  $d$  band in the alloy while the other electron has gone into the Cu conduction band.

The spatial dependence of  $\sigma(r, T)$  is also compared to the calculation of Alloul, Darville, and Bernier.<sup>17</sup> Their calculation agrees well with our data only if the identifications of satellites  $B$  and  $C$  are reversed. However, this is not allowed by Stakelon's identification of  $B$  as the third neighbor.

It is also determined that the magnetization in the electron gas is aligned antiferromagnetically with the moment on the Fe and is about nine times smaller. This agrees with the neutron-diffraction studies<sup>15</sup> and with perturbation-theory calculations. Also our satellite data agree fairly well with the average Knight shift obtained by Gardner and Flynn<sup>40</sup> in molten CuFe.

To comment on the Kondo effect, the satellite shifts were measured as a function of temperature to below  $T_K$ . The shifts of each of the four

satellites measured scaled as  $\chi(T) \sim 1/(T+29)$ . Thus we conclude that

$$\sigma(r, T)/H = \chi(T)f(r) \quad (1)$$

describes the spin density of CuFe both above and below  $T_K$ . So there is no shape change or enhancement of the conduction-electron spin density, and no spin compensating state forms below  $T_K$ . The Kondo effect exhibits itself only in the magnetic-to-nonmagnetic transition of the bulk susceptibility as  $T$  is lowered below  $T_K$  and not in an enhancement or a shape change of  $\sigma(r, T)$ .

An argument is presented to show that the low-temperature anomaly in the NMR linewidth is due to interactions. The linewidths due to single impurities then agrees with Eq. (1). Such a conclusion has also been arrived at in the recent NMR linewidth experiments.<sup>17</sup> Also the Mössbauer results<sup>14</sup> support Eq. (1) if the data of each of the three Mössbauer experiments are analyzed separately. Then all experiments agree with Eq. (1).

#### ACKNOWLEDGMENTS

We would like to thank Mr. T. Stakelon for assistance in sample preparation and permission to quote his single-crystal results. In addition, we gratefully acknowledge the assistance of Mr. T. Aton and Mr. J. Crues in collecting some of the high-temperature data and thank Professor T. Rowland for the use of his wide-line spectrometer.

\*Research supported in part by the Energy Research and Development Administration under Contract No. AT(11-1)-1198.

†Present address: Xerox Palo Alto Research Center, Palo Alto, Calif. 94304.

<sup>1</sup>A thorough review of the magnetic properties of metallic alloys has appeared in *Magnetism*, edited by H. Suhl (Academic, New York, 1973), Vol. 5.

<sup>2</sup>J. Kondo, in *Solid State Physics*, edited by H. Ehrenreich, F. Seitz, and D. Turnbull (Academic, New York, 1969), Vol. 23.

<sup>3</sup>A. Narath, *Crit. Rev. Solid State Sci.* **3**, 1 (1972).

<sup>4</sup>A. J. Heeger, in *Solid State Physics*, edited by H. Ehrenreich, F. Seitz, and D. Turnbull (Academic, New York, 1969), Vol. 23.

<sup>5</sup>J. L. Tholence and R. Tournier, *Phys. Rev. Lett.* **25**, 867 (1970).

<sup>6</sup>E. Müller-Hartmann, *Z. Phys.* **223**, 277 (1969).

<sup>7</sup>A. J. Heeger, L. B. Welsh, M. A. Jensen, and G. Gladstone, *Phys. Rev.* **172**, 302 (1968).

<sup>8</sup>P. E. Bloomfield, R. Hecht, and P. R. Sievert, *Phys. Rev. B* **2**, 3714 (1970).

<sup>9</sup>M. S. Fullenbaum and D. S. Falk, *Phys. Rev.* **157**, 452 (1967); H. U. Everts and B. N. Ganguly, *ibid.* **174**, 594 (1968).

<sup>10</sup>P. Jena and D. J. W. Geldart, *Phys. Rev. B* **7**, 439

(1973).

<sup>11</sup>H. Alloul, *J. Phys. F* (to be published).

<sup>12</sup>D. C. Golibersuch and A. J. Heeger, *Phys. Rev.* **182**, 584 (1969).

<sup>13</sup>J. E. Potts and L. B. Welsh, *Phys. Rev. B* **5**, 3421 (1972).

<sup>14</sup>P. Steiner, W. v. Zdrojewski, D. Gumprecht, and S. Hüfner, *Phys. Rev. Lett.* **31**, 355 (1973).

<sup>15</sup>C. Stassis and C. G. Shull, *Phys. Rev. B* **5**, 1040 (1972).

<sup>16</sup>H. Nagasawa and W. A. Steyert, *J. Phys. Soc. Jpn.* **28**, 1202 (1970).

<sup>17</sup>H. Alloul, J. Darville, and P. Bernier, *J. Phys. F* (to be published).

<sup>18</sup>J. B. Boyce and C. P. Slichter, *Phys. Rev. Lett.* **32**, 61 (1972).

<sup>19</sup>H. Alloul, P. Bernier, H. Launois, and J. P. Pouget, *J. Phys. Soc. Jpn.* **30**, 101 (1971).

<sup>20</sup>D. C. Lo, D. V. Lang, J. B. Boyce, and C. P. Slichter, *Phys. Rev. B* **8**, 973 (1973).

<sup>21</sup>D. V. Lang, J. B. Boyce, D. C. Lo, and C. P. Slichter, *Phys. Rev. Lett.* **29**, 776 (1972); D. V. Lang, D. C. Lo, J. B. Boyce, and C. P. Slichter, *Phys. Rev. B* **9**, 3077 (1974).

<sup>22</sup>J. B. Boyce, T. J. Aton, and C. P. Slichter, *AIP Conf. Proc.* **18**, 252 (1974).

<sup>23</sup>N. Karnezos and J. A. Gardner, *Phys. Rev. B* **9**, 3106

- (1974).
- <sup>24</sup>K. Tompa, *Phys. Status Solidi* **62**, 265 (1974).
- <sup>25</sup>H. Takenaka, Y. Oda, and K. Asayama, *J. Phys. Soc. Jpn.* (to be published).
- <sup>26</sup>T. Sugawara, *J. Phys. Soc. Jpn.* **14**, 643 (1959).
- <sup>27</sup>R. B. Frankel, N. A. Blum, B. B. Schwartz, and D. J. Kim, *Phys. Rev. Lett.* **18**, 1050 (1967); T. A. Kitchens, W. A. Steyert, and R. D. Taylor, *Phys. Rev.* **138**, A467 (1965).
- <sup>28</sup>I. A. Campbell, *Phys. Rev. B* **10**, 4036 (1974).
- <sup>29</sup>P. Steiner and S. Hufner, *Phys. Rev. B* **10**, 4038 (1974).
- <sup>30</sup>P. Steiner, S. Hufner, and W. D. Zdrojewski, *Phys. Rev. B* **10**, 4704 (1974).
- <sup>31</sup>K. D. Schotte and U. Schotte, *Phys. Rev. B* **4**, 2228 (1971).
- <sup>32</sup>C. M. Hurd, *J. Phys. Chem. Solids* **28**, 1345 (1967).
- <sup>33</sup>P. Bernier and H. Alloul, *J. Phys. F* **3**, 869 (1973); H. Alloul and P. Bernier, *ibid.* **4**, 870 (1974).
- <sup>34</sup>B. Giovannini and A. J. Heeger, *Solid State Commun.* **7**, 287 (1969).
- <sup>35</sup>H. Benoit, P. G. de Gennes, and D. Silhouette, *C. R. Acad. Sci. (Paris)* **256**, 3841 (1963).
- <sup>36</sup>M. D. Daybell and W. A. Steyert, *Rev. Mod. Phys.* **40**, 380 (1968).
- <sup>37</sup>A. Blandin, *J. Appl. Phys.* **39**, 1285 (1968).
- <sup>38</sup>E. Daniel and J. Friedel, in *Proceedings of the Ninth International Conference on Low-Temperature Physics*, edited by J. G. Daunt, D. O. Edwards, F. J. Milford, and M. Yaquub (Plenum, New York, 1965), p. 933.
- <sup>39</sup>D. Pines, in *Solid State Physics*, edited by F. Seitz and D. Turnbull (Academic, New York, 1955), Vol. 1, p. 367.
- <sup>40</sup>J. A. Gardner and C. P. Flynn, *Philos. Mag.* **15**, 1233 (1967).